Published in final edited form as:
J Am Chem Soc. 2010 October 13; 132(40): 14015–14017. doi:10.1021/ja106432h.

The Structure of Formaldehyde-Inhibited Xanthine Oxidase Determined by 35 GHz ^{2}H ENDOR Spectroscopy

Muralidharan Shanmugam[†], **Bo Zhang**[‡], **Rebecca L. McNaughton**[†], **R. Adam Kinney**[†], **Russ Hille**[‡], and **Brian M. Hoffman**[†,*]

[†]Chemistry Department, Northwestern University, Evanston, Illinois, 60208-3113

[‡]Department of Biochemistry, University of California, Riverside, California-95521

Abstract

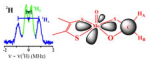

The formaldehyde-inhibited Mo(V) state of xanthine oxidase (**I**) has been studied for four decades, yet it has not proven possible to distinguish unequivocally among the several structures proposed for this form. The uniquely large isotropic hyperfine coupling for ^{13}C from CH_2O led to the intriguing suggestion of a direct Mo-C bond for the active site of **I**. This suggestion was supported by the recent crystal structures of glycol- and glycerol-inhibited forms of aldehyde oxidoreductase (AOR), a member of the xanthine oxidase family. ^{1,2}H-ENDOR spectra of **I**($C^{1,2}H_2O$) in H_2O/D_2O buffer now unambiguously reveal that the active-site structure for **I** contains a CH_2O adduct of Mo(V) in the form of a four-membered ring with S and O linking the C to Mo, and rule out a direct Mo-C bond. DFT computations are consistent with this conclusion. We interpret the large ^{13}C coupling as resulting from a 'transannular hyperfine interaction'.

Xanthine oxidase is a molybdo-enzyme that catalyses the oxidative hydroxylation of a variety of heterocyclic and aldehyde substrates, including the physiological substrates hypoxanthine and xanthine.1 Of the large number of EPR-active Mo(V) intermediates exhibited by this enzyme,2 one of the most intriguing is the CH_2O inhibited Mo(V) form (**I**) first described by Bray and coworkers.3 Its most remarkable feature, revealed by Howes et al., is the presence of a carbon derived from CH_2O that EPR and ENDOR spectroscopies show to have a uniquely large ^{13}C isotropic hyperfine coupling, a_{iso} (^{13}C) ~ 43.0 MHz.4,5 This value contrasts with the five-fold smaller coupling for the Mo-O- ^{13}C of the "2-hydroxy-6-methyl-purine (HMP) very rapid" form (a_{iso} = 7.9 MHz).6 Although **I** has been studied for 40 years, it has not proven possible to distinguish unequivocally among the viable candidates for its structure (Scheme 1).5,7–13

The large isotropic ^{13}C hyperfine coupling for **I** led Howes et al. to the intriguing suggestion that it contains a CHO fragment with a direct Mo-C bond, Scheme 1, **C**.4,5 This suggestion recently received support from the crystal structures of glycol and glycerol inhibited forms of aldehyde oxidoreductase (AOR), a member of the xanthine oxidase family.7 These structures exhibit Mo-C bond distances of 2.36 Å and 2.72 Å, respectively, the former in particular being suggestive of direct Mo-C bonding interactions. In contrast, analysis of the smaller ^{13}C coupling for a substrate-derived species bound to Mo(V) of the "very rapid"

* bmh@northwestern.edu .

Supporting Information Available: One EPR figure; one ENDOR figure; DFT calculation methods.

state of xanthine oxidase indicated there was no direct Mo-C bond,6 and this was confirmed by recent crystal structures for that intermediate.14,15

We here report that ^{1,2}H-ENDOR spectra of **I**($C^{1,2}H_2O$) prepared16 in H_2O/D_2O buffer rule out all models proposed for the active-site structure of **I** (Scheme 1) except for model **A**, a four-membered cyclic adduct of CH_2O with S and O linking the C to Mo. DFT calculations are consistent with the ENDOR finding that **A** represents the structure for the active site of **I**, and not the direct Mo-C bond of **C**.

The X-band EPR spectrum of **I**($^{12,13}C^1H_2O$) in H_2O shows a doublet splitting from the ^{13}C-nucleus, with each line further split into a doublet from a single proton that derives from CH_2O.4 The 35 GHz echo-detected EPR spectrum of **I**($^{12,13}C^1H_2O$) in H_2O show the ^{13}C doublet from $^{13}C^1H_2O$, but the ^{1}H splitting is not observed, Fig S1.17,18 The EPR spectrum of **I**($^{12,13}C^1H_2O$) further shows hyperfine splitting from ^{95,97}Mo (natural abundance: 15.9% ^{95}Mo; 9.6% ^{97}Mo). The g_1 and g_3 splittings are observable in both X and Q band spectra; those associated with g_2 are only resolved at Q-band (Fig S1). Simulations of the EPR spectra gave principal g-values and $\boldsymbol{A}$ for the ^{13}C of CH_2O that agree with those of Howes *et al*.: **g** = [1.988, 1.974, 1.948], $\boldsymbol{A}$(^{13}C) = [51.5, 40, 40] MHz, a_{iso} = 43.8 MHz.

Fig 1 presents 35 GHz Davies ^{1}H and ^{95,97}Mo (*upper*), and Mims ^{2}H (*lower*) ENDOR spectra collected for **I**($^{12}C^{1,2}H_2O$) in H_2O/D_2O near g_2, the magnetic field corresponding to the maximum EPR intensity. The Davies spectra of **I**(C^1H_2O) in H_2O and D_2O are essentially the same (**A**), both exhibiting a ^{1}H doublet centered at the ^{1}H-nuclear Larmor frequency and split by $A \approx 13$ MHz. This doublet is absent in the spectrum of **I**(C^2H_2O) in H_2O (**B**) and thus is associated with a proton, ^1H_A, derived from CH_2O. The ^{1}H doublet in Fig 1 rides on ^{95,97}Mo-ENDOR signals and is more clearly seen upon subtraction of the spectrum of **I**(C^2H^2O, **B**) from that of **I**(C^1H_2O, **A**), spectrum **A**–**B**. The ^1H_A doublet is replaced by a corresponding ^2H_A signal when C^2H_2O is the substrate. Davies ^{2}H-ENDOR spectra of **I**(C^2H_2O) in H_2O exhibit a ^2H_A doublet without resolved quadrupole splitting (not shown). The hyperfine interaction, $\boldsymbol{A}$(^2H_A) corresponds to a smaller value of $\boldsymbol{A}$(^1H_A) than that seen directly in the ^{1}H-ENDOR spectrum of **I**(C^1H_2O) in H_2O/D_2O because of a substantial isotope effect on the hyperfine couplings.19,20

To test for both exchangeable and non-exchangeable ^{2}H signal(s) with smaller hyperfine couplings than $^{1,2}H_A$, Mims ^{2}H-ENDOR spectra were collected for **I**(C^1H_2O) in D_2O and **I**(C^2H_2O) in H_2O at g_2 (Fig 1, *lower*). The nearly featureless ^{2}H spectrum of **I**(C^1H_2O) in D_2O shows clearly that there are no exchangeable protons in the active site of **I**. However, the ^{2}H spectrum of **I**(C^2H_2O) in H_2O shows *two* doublets from deuterons derived from the C^2H_2O (Fig 1). The larger coupling corresponds to ^2H_A observed in the Davies ^{1}H-ENDOR spectra of **I**(C^1H_2O) in H_2O/D_2O, again with the isotope effect on the hyperfine coupling. The second doublet in the Mims spectrum for **I**(C^2H_2O) also does not exchange in H_2O buffer, and thus corresponds to the *second* C–H deuteron introduced with the C^2H_2O, denoted ^2H_B.

To confirm that the Mims ^{2}H spectrum is not significantly distorted by suppression `holes' associated with this technique21 and to determine the ^{2}H hyperfine and quadrupolar tensors, we collected a complete 2-D field-frequency ^{2}H-ENDOR pattern of spectra acquired at numerous magnetic fields across the EPR envelope and simulated this pattern with inclusion of the suppression effects (Fig S2).22 At magnetic fields near g_1, the spectra show the ^2H_A and ^2H_B doublets centered at ^{2}H-Larmor frequency and split by $A \sim 1.8$ MHz and 0.4 MHz respectively. The ^{2}H-ENDOR pattern does not change significantly as the field is moved towards g_2 and g_3, except in intensity, indicating that the hyperfine couplings of ^2H_A and ^2H_B are largely isotropic. The 2-D pattern is well simulated by the 1:1 summation of

simulations of $^{2}H_A$ and $^{2}H_B$, with, $\boldsymbol{A}(^{2}H_A)$ = [1.8, 1.8, 1.9] MHz; $\boldsymbol{A}(^{2}H_B)$ = [0.44, 0.4, 0.39] MHz. Neither ^{2}H exhibits quadrupolar splitting (I = 1) because of the large ENDOR line widths. As noted above for the g_2 spectrum, the tensor obtained from simulations of the $^{2}H_A$-ENDOR pattern only approximately matches that obtained by fitting a 2-D ^{1}H Davies ENDOR pattern for $^{1}H_A$ because of an isotope effect on the hyperfine couplings.19,20

The observation that both aldehydic protons of CH_2O are non-exchangeably hyperfine-coupled to the Mo(V) of **I** rules out all candidates in Scheme 1 for the active-site structure of **I** except the cyclic CH_2O adduct, **A**.

DFT calculations are consistent with experiment in showing a large a_{iso} for the ^{13}C. of Model **A**. This model yielded hyperfine tensors for ^{13}C, $^{2}H_A$ and $^{2}H_B$ of CH_2O that all are in satisfactory agreement with the experimentally observed values: $a_{iso}(^{13}C)$ ~ 47.9 MHz, $\boldsymbol{A}(^{13}C)$ = [53.6, 45.4, 44.6] MHz; $\boldsymbol{A}(^{2}H_A)$ = [4.0, 3.3, 3.0] MHz, $\boldsymbol{A}(^{2}H_B)$ = [0.38, −0.67, −0.72] MHz. Most importantly, the carbon-bound CHO complex, model **C**, already ruled out by the absence of H_B, is calculated to have almost three-fold and five-fold smaller ^{13}C and $^{1}H_A$ hyperfine couplings, respectively: a^{iso} (^{13}C) = ~ 16.1 MHz, $\boldsymbol{A}(^{13}C)$ = [23.2, 13.4, 11.7] MHz; $\boldsymbol{A}(^{2}H_A)$ = [0.51, −0.43, −0.66] MHz.

Why is the ^{13}C coupling so large for the carbon of CH_2O that is not directly coordinated to Mo(V) in the four-membered ring of model **A**, and not for the carbon directly bonded to the metal ion in **C**? We interpret this as resulting from a `transannular hyperfine interaction'.23,24 The carbon is in line with a lobe of the half-occupied Mo(d_{xy}) orbital, and this allows overlap between Mo(d_{xy}) and orbitals of carbon; the large a_{iso} for ^{13}C corresponds to only ~ 1.2% spin density in a carbon 2s orbital. Analogous behavior was first observed for a phosphorous atom that formed part of four membered cyclic structures of Mo(V) and V(IV) with dialkyl/aryldithio-phosphinato ligands.23,24 A weaker hyperfine coupling was observed when the 31P is bound to the metal-ion directly through a monodentate M-O-P linkage.25 Such considerations may have relevance to a recent proposal of a direct Fe-C bond based on a large ^{13}C coupling.26

Finally, regarding the use of distances in the X-ray structure to infer a direct Mo-C bond, we note that the DFT-optimized cyclic structure **A** has a Mo-C distance of 2.76 Å, the same as found by x-ray diffraction for the glycerol-inhibited form of AOR.7

Supplementary Material

Refer to Web version on PubMed Central for supplementary material.

Acknowledgments

Support by the NIH (GM 075036, RH) and NSF (MCB0723330, BMH).

REFERENCES

(1). Hille R. Chemical Reviews (Washington, D. C.). 1996; 96:2757–2816.

(2). Hille, R. In Metals in Biology: Applications of High-Resolution EPR to Metalloenzymes. In: Hanson, G.; Berliner, L.; J., editors. Vol. Vol. 29. Springer; Berlin: 2010. p. 91-121.

(3). Pick FM, McGartoll MA, Bray RC. Eur. J. Biochem. 1971; 18:65–72. [PubMed: 4322209]

(4). Howes BD, Bennett B, Bray RC, Richards RL, Lowe DJ. J. Am. Chem. Soc. 1994; 116:11624–11625.

(5). Howes BD, Bray RC, Richards RL, Turner NA, Bennett B, Lowe D. J. Biochemistry. 1996; 35:1432–1443.

(6). Manikandan P, Choi E-Y, Hille R, Hoffman BM. J. Am. Chem. Soc. 2001; 123:2658–2663. [PubMed: 11456936]

(7). Santos-Silva T, Ferroni F, Thapper A, Marangon J, Gonzalez PJ, Rizzi AC, Moura I, Moura JJG, Romao MJ, Brondino CD. J. Am. Chem. Soc. 2009; 131:7990–7998. [PubMed: 19459677]

(8). Metz S, Wang D, Thiel W. J. Am. Chem. Soc. 2009; 131:4628–4640. [PubMed: 19290633]

(9). Zhang X-H, Wu Y-D. Inorg. Chem. (Washington, DC, U. S.). 2005; 44:1466–1471.

(10). Amano T, Ochi N, Sato H, Sakaki S. J. Am. Chem. Soc. 2007; 129:8131–8138. [PubMed: 17564439]

(11). Howes BD, Pinhal NM, Turner NA, Bray RC, Anger G, Ehrenberg A, Raynor JB, Lowe D. J. Biochemistry. 1990; 29:6120–6127.

(12). Morpeth FF, Bray RC. Biochemistry. 1984; 23:1332–1338. [PubMed: 6546882]

(13). Turner NA, Bray RC, Diakun GP. Biochem. J. 1989; 260:563–571. [PubMed: 2764889]

(14). Pauff JM, Zhang J, Bell CE, Hille R. J. Biol. Chem. 2008; 283:4818–4824. [PubMed: 18063585]

(15). Pauff JM, Cao H, Hille R. J. Biol. Chem. 2009; 284:8760–8767. [PubMed: 19109252]

(16). Xanthine oxidase was prepared from unpasteurized milk as described by Massey et al (1969). 2H and 13C-labeled H2CO were from Cambridge Isotopes, D2O from Isotec, Inc. 35 GHz pulsed EPR and ENDOR spectra were obtained as described by Lees et al. (2009)

(17). Massey V, Brumby PE, Komai H, Palmer G. J. Biol. Chem. 1969; 244:1682–1691. [PubMed: 5813728]

(18). Lees NS, Hänzelmann P, Hernandez HL, Subramanian S, Schindelin H, Johnson MK, Hoffman BM. J. Am. Chem. Soc. 2009; 131:9184–9185. [PubMed: 19566093]

(19). Weber S, Kay CWM, Bacher A, Richter G, Bittl R. ChemPhysChem. 2005; 6:292–299. [PubMed: 15751352]

(20). Kinney RA, Hetterscheid DGH, Hanna BS, Schrock RR, Hoffman BM. Inorg. Chem. (Washington, DC, U. S.). 2010; 49:704–713.

(21). Schweiger, A.; Jeschke, G. Principles of Pulse Electron Paramagnetic Resonance. Oxford University Press; Oxford, UK: 2001.

(22). Doan PE, Lees NS, Shanmugam M, Hoffman BM. Appl. Magn. Res. 2010; 37:763–779.

(23). Stiefel EI, Newton WE, Pariyadath NJ. Less-Common Met. 1977; 54:513–525.

(24). Miller GA, McClung RED. Inorg. Chem. (Washington, DC, U. S.). 1973; 12:2552–2561.

(25). Gelmini L, Stephan DW. Organometallics. 1987; 6:1515–1522.

(26). Wang W, Wang K, Liu Y-L, No J-H, Li J, Nilges MJ, Oldfield E. Proc. Natl. Acad. Sci. U. S. A. 2010:1–6. Early Edition.

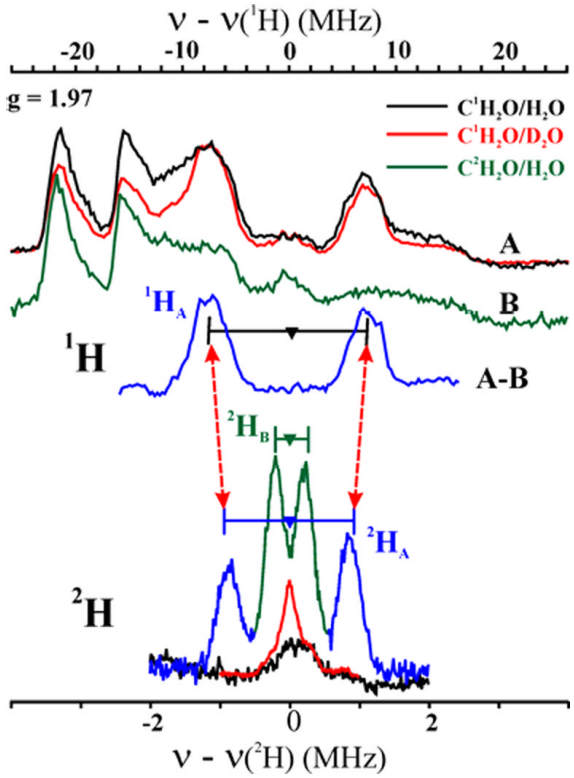

Figure 1.

35 GHz (*Upper*) Davies ^{1}H and ^{95,97}Mo (**A**, **B**), ENDOR spectra of **I**($C^{1,2}H_2O$) in H_2 and D_2O buffer. (*Lower*) Mims ^{2}H spectra of **I**($C^{2}H_2O$) in H_2O (*green/blue*), **I**($C^{1}H_2O$) in H_2O and D_2O buffer. Horizontal bars indicate hyperfine splittings for $^{1,2}H_{A,B}$ non-exchangeable protons. *Conditions: g* = 1.97; T = 2 K. *Davies*: π-pulse = 80 ns, τ = 600 ns, repetition time = 50 ms, 34.84 GHz; *Mims*, ^{2}H: *π/2* pulse = 50 ns, τ = 800 ns, repetition time = 50 ms, 34.87 GHz.

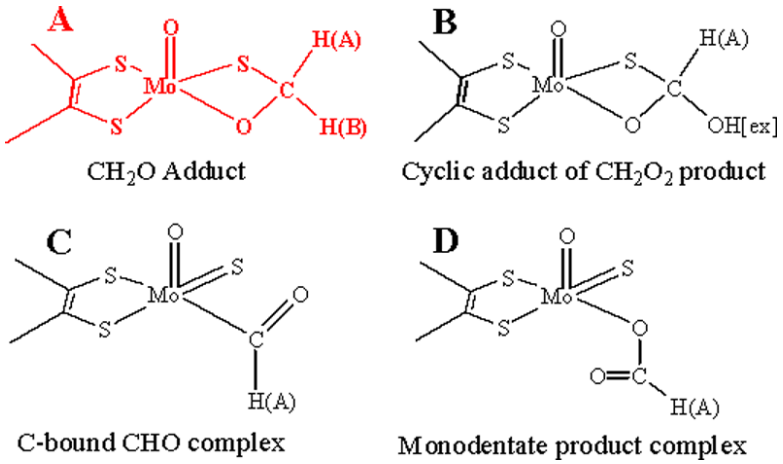

Scheme 1.